Computers & Industrial Engineering 2026, http://dx.doi.org/10.1016/j.cie.2026.112389

User preference-based energy management strategy for EV charging infrastructure

Wenjie Hu [a], Jiamou Su [a], Yang Wang [a,*], Ya-Hui Jia [b], Wei-Neng Chen [c], Jin-Kao Hao [d]

[a] *School of Management, Northwestern Polytechnical University, 710072 Xi'an, China*

[b] *School of Future Technology, South China University of Technology, 510641 Guangzhou, China*

[c] *School of Computer Science and Engineering, South China University of Technology, 510006 Guangzhou, China*

[d] *Department of Computer Science, Université d'Angers, 49045 Angers, France*

Abstract

In this paper, we address a new user preference-based energy management (UPEM) problem for an electric vehicle (EV) charging station with battery energy storage system (BESS). The UPEM problem accounts for time-sensitive and price-sensitive user preferences, using a fuzzy logic controller to describe the behavior of price-sensitive users. By considering time-of-use electricity pricing and introducing vehicle-to-grid (V2G) technology, the UPEM problem aims to minimize charging station operating costs by optimizing EV and BESS charging and discharging powers, while determining the BESS's optimal capacity. To address the UPEM problem, we employ a rolling horizon approach to decompose the dynamic problem into a series of static subproblems, and propose a hybrid metaheuristic algorithm to solve each static subproblem. Specifically, the hybrid metaheuristic algorithm includes a greedy procedure for EV charging and discharging schedules and a particle swarm optimization (PSO) procedure enhanced with dominance-based correction rules for BESS charging and discharging schedule. We generate five simulation scenarios to model different numbers of EVs and average parking durations for experimentations. Results reveal that our greedy algorithm alone achieves an average cost reduction of 22.91% compared to the state-of-the-art algorithm in the literature. In addition, our proposed hybrid metaheuristic algorithm consistently outperforms scheduling rules commonly applied in practice across all scenarios, delivering improvements from 18.60% to 68.72%. Comparative

* Corresponding authors.
Email addresses: huwenjie@mail.nwpu.edu.cn (Wenjie Hu), sujiamou@mail.nwpu.edu.cn (Jiamou Su), yangw@nwpu.edu.cn (Yang Wang), jia.yahui@foxmail.com (Ya-Hui Jia), cschenwn@scut.edu.cn (Wei-Neng Chen), jin-kao.hao@univ-angers.fr (Jin-Kao Hao)

experiments with other metaheuristic algorithms further demonstrate the superiority of the proposed hybrid metaheuristic algorithm in terms of solution quality and computational efficiency.

Keywords: electric vehicles; charging station; energy management; battery energy storage system; hybrid metaheuristic

1. Introduction

With the gradual depletion of fossil fuel resources and the increasing global concern for environmental protection, more people are opting for electric vehicles (EVs) as their mode of transportation (Yuan et al., 2020; Zhang et al., 2018; Zhu et al., 2019). However, the large-scale integration of EVs into the power grid introduces numerous technical challenges, particularly by imposing higher energy demand for the power system, which may in turn affect grid stability and quality (Çakıl & Aksoy, 2025; Mahmud et al., 2023). To address this issue, time-of-use electricity pricing policies have emerged as an effective regulatory measure that guide users to schedule charging times rationally and mitigate load fluctuations across different periods (Christensen et al., 2020; Yang et al., 2020; Zhou et al., 2019). In the context of time-of-use pricing, more and more studies have focused on energy management of EV charging stations. In particular, considerable attention has been paid to EV charging scheduling and the incorporation of vehicle-to-grid (V2G) technology and/or battery energy storage systems (BESS) (Hannan et al., 2017; Lai et al., 2022; Bibak & Tekiner-Moğulkoç, 2021; Abdelfattah et al., 2024).

Determining the optimal capacity of BESS and the charging and discharging powers for both EVs and BESS through optimization algorithms can significantly reduce the operational costs of charging stations (Bhatti et al., 2019; Dai et al., 2019; Mohamed & Mohammed, 2013). However, most existing studies treat BESS sizing and energy management as separate problems, determining the capacity first and then planning the energy management strategy, instead of integrating the two. This separate treatment may limit the effectiveness of BESS and prevent its full potential from being realized. On the other hand, user demand also plays a critical role in energy management strategies. While many studies have considered user behavior, such as

charging time and duration (Domínguez-Navarro et al., 2019; Guner & Ozdemir, 2017; Mohamed et al., 2014), user preferences have not been adequately addressed. For example, user preferences regarding desired state-of-charge (SOC) increments under different electricity prices are often overlooked. This gap may lead to unmet charging demand and lower user satisfaction, making users less likely to return for future charging, which directly reduces the station's revenue. Therefore, it is crucial to develop effective energy management strategy that fully account for user preferences while optimizing the utilization of V2G and BESS at EV charging station.

In this paper, we address a new user preference-based energy management (UPEM) problem for an electric vehicle charging station and propose a rolling horizon approach for handling the uncertain arrivals of EVs. The main contributions of this work can be summarized as follows:

1. We consider both time-sensitive and price-sensitive users. Time-sensitive users are charged at maximum power to minimize their waiting time, while price-sensitive users adjust their charging demand based on electricity prices. V2G technology is further employed to reduce overall charging costs.
2. We embed BESS capacity decisions into real-time energy management, ensuring that storage sizing consistently aligns with charging and discharging needs, thereby improving the economic efficiency of the charging station.
3. We implement a rolling horizon approach and develop a hybrid metaheuristic that uses a greedy strategy for EV scheduling based on electricity prices and a PSO-based method for BESS scheduling, enhanced with dominance-based correction rules to improve solution quality.
4. We validate the proposed framework through extensive computational experiments. The greedy algorithm is compared with existing methods to demonstrate its effectiveness, while the hybrid metaheuristic algorithm is evaluated against commonly used scheduling rules and established metaheuristics, including the genetic algorithm and simulated annealing. Statistical analyses further confirm the superiority of the proposed approach in

terms of solution quality. Evaluations across diverse scenarios with varying user numbers and parking durations highlight the flexibility and adaptability of the proposed method.

The rest of this paper is organized as follows: Section 2 summarizes the related work in the literature. Section 3 describes the overall architecture of the electric vehicle charging station studied in this work and formulates user preferences, objective functions, and system constraints using mathematical expressions. Section 4 outlines the algorithmic framework and details the process of the hybrid metaheuristic algorithm. Section 5 presents the experimental study and analyzes the results. Finally, Section 6 concludes the paper.

2. Related work

Energy management in electric vehicle charging stations is influenced by various factors, including different forms of uncertainty—such as arrival and departure times—as well as energy supply infrastructure types and electric vehicle charging demands. Researchers have examined these factors from different perspectives, each emphasizing specific aspects.

2.1 Uncertainties in the EV charging station

There are numerous uncertainties in the operation of EV charging station, such as EV arrival and departure time, which increase the complexity of charging station operation management (Feng et al., 2020; Jia et al., 2023). Li et al. (2020) considers the stochastic arrival and departure times of EVs and dynamically adjusted the charging and discharging power of different vehicles using a priority rule to reduce charging costs. Viegas et al. (2021) considers random charging demands and time-of-use electricity prices and employed a fuzzy logic control method for real-time decision-making on EV charging and discharging power. Liu et al. (2016) focused on energy management optimization at PV-assisted charging stations, requiring users to set target energy levels and departure times to reduce demand uncertainty, while simultaneously considering the uncertainties of electricity price and solar irradiance. They solved the

problem using a real-time online algorithm that combines online learning with rule-based methods. García-Álvarez et al. (2018) examined the EV charging cycle scheduling problem by considering the random arrival and departure times and charging demands of EVs. They decomposed the dynamic problem into a series of static problems over fixed time intervals, and then solved it by using a memetic algorithm. Pan et al. (2024) proposed a rolling optimization strategy that combines the particle swarm optimization algorithm and the gravitational search algorithm to tackle uncertainties in EV arrival times. Their strategy develops real-time charging and discharging schedule based on the states of EVs connected to the grid at each time instant.

2.2 Energy supply facilities

Energy supply facilities (such as BESS, V2G, and renewable energy generators) in EV charging station have also garnered significant attention from researchers, as they can reduce grid load fluctuations and operational costs (Alaee et al., 2023). Bhatti et al. (2019) proposed a rule-based method to determine the sizing of photovoltaic (PV) arrays and BESS. Their approach dynamically adjusts the power of PV arrays and BESS, prioritizing the utilization of cost-effective PV-generated electricity. Dai et al. (2019) developed a multi-agent particle swarm optimization algorithm to solve the scheduling problem of an EV charging station with a BESS and a small-scale PV system. Their results demonstrated that PV and BESS can effectively reduce both the construction and operational costs of the charging station. Mohamed et al. (2013) addressed power scheduling in grid-connected microgrids that integrate PV, wind turbines, and BESS. They proposed a rule-based control algorithm that prioritizes renewable energy to meet load demand. Furthermore, when renewable generation is insufficient, the BESS output power is determined based on its current state and forecasts of grid load over the next few hours. Honarmand et al. (2014) formulated a nonlinear programming model for EV power scheduling with V2G technology. By constructing a relationship model between battery lifespan and the number of charge-discharge cycles, they aimed to maximize discharging revenue while ensuring limited battery degradation.

2.3 EV charging demand

Modeling EV charging demand is also crucial for the charging and discharging scheduling problem. The characteristics of user energy demand and its temporal distribution pose challenges to the adaptability of scheduling algorithms. Guner et al. (2017) constructed EV charging demand using sequential Monte Carlo simulation based on real-world data on EV arrival and departure times, as well as probabilistic parameters related to driver behavior. They determined the appropriate capacity of the BESS at the charging station. Mohamed et al. (2014) estimated arrival and departure times based on users' daily travel distances and per-kilometer energy consumption. They developed a power demand model and managed charging and discharging time using a fuzzy logic controller. Domínguez-Navarro et al. (2019) modeled EV arrival times using an exponential distribution with varying parameters for each hour to accurately capture the complexity and variability of user demand, and proposed a genetic algorithm to solve the scheduling problem. Aliasghari et al. (2018) established a demand response model to encourage EV users to manage their consumption based on electricity prices by shifting or reducing their load during high-price periods. They formulated a stochastic programming model to solve the problem. Yao et al. (2017) tackled real-time optimization of EV charging plans by incorporating user preferences for electricity prices. They proposed a demand response model to enhance user satisfaction and applied convex relaxation methods.

2.4 Summary

The existing literature on EV charging station scheduling addresses key challenges from three interconnected perspectives: uncertainty handling, energy supply integration, and user demand modeling. Research on operational uncertainties primarily focuses on dynamic and stochastic factors such as EV arrival and departure times, random charging demands, and fluctuating electricity prices. To manage these complexities, scholars have proposed adaptive scheduling strategies based on real-time optimization, priority rules, fuzzy logic, and evolutionary algorithms. In parallel, studies on energy supply emphasize the integration of PV systems, BESS, and V2G technologies to improve

energy self-sufficiency and cost efficiency. These works typically employ rule-based and optimization-based approaches to coordinate hybrid energy sources, aiming to balance load demand and prolong battery lifespan. Finally, research on demand modeling aims to accurately capture user behavior and energy needs through stochastic simulations, probabilistic distributions, and behavioral models. These models serve as critical inputs for scheduling algorithms and are often embedded within broader optimization frameworks to support real-time decision-making and demand response. A summary of representative studies from these perspectives is provided in Table 1.

Table 1 Summary of representative studies on EV charging station energy management

Reference	**Uncertainty considered**	**Energy supply facilities**	**EV demand modeling**	**Solution approach**
Mohamed et al. (2013)	Renewable generation uncertainty	PV, wind, BESS	—	Rule-based control
Honarmand et al. (2014)	—	V2G	—	Nonlinear programming
Liu et al. (2016)	Electricity price, solar irradiance, demand uncertainty	PV	User target energy and departure time	Online learning + rule-based method
Yao et al. (2017)	Demand response	—	EV charging demand	Convex relaxation
García-Álvarez et al. (2018)	EV arrival/departure time, charging demand	—	—	Memetic algorithm
Dai et al. (2019)	—	PV, BESS	EV charging pattern simulation	Multi-agent PSO
Domínguez-Navarro et al. (2019)	EV arrival time	Wind, PV, BESS	Monte Carlo simulation	Genetic algorithm
Li et al. (2020)	PV generation uncertainty, electricity price, user energy requirements	PV, BESS, V2G	User energy requirements	Chance-constrained programming
Viegas et al. (2021)	Charging demand, electricity price	V2G	—	Fuzzy logic control
Pan et al. (2024)	—	V2G	—	PSO + gravitational search algorithm
This study	EV arrival/departure, electricity price	BESS, V2G	User preference and charging demand	Greedy + PSO

Although existing studies have made significant progress in EV charging station scheduling, several challenges remain. Many studies focus on individual aspects of charging station operation, while the joint consideration of uncertainties, energy supply

facilities, and EV demand characteristics remains limited. Moreover, existing works involving PV, BESS, and V2G mainly emphasize energy coordination or planning, whereas efficient real-time optimization of continuous charging and discharging decisions is still challenging. To address these issues, this study develops a rolling horizon hybrid optimization framework that integrates a greedy strategy and PSO for coordinated EV and BESS scheduling.

3. Problem formulation

Our UPEM problem focuses on energy management strategy for EVs and a BESS within a charging station. The objective is to minimize operational costs by optimizing the charging and discharging powers of EVs and the BESS across different time periods throughout the day. Additionally, the optimal capacity of the BESS is determined based on a simulation of the optimized charging and discharging schedule. The architecture of the charging station, shown in Figure 1, includes EVs, a BESS, and an energy management system (EMS), along with a connection to the power grid, which supports the station externally. In this figure, solid arrows indicate energy flows, while dashed arrows represent information flows. From the perspective of energy flow, the main interactions occur among the power grid, EVs, and the BESS. Specifically, G2V (power grid to EVs) denotes the standard charging mode where the power grid supplies power to EVs. V2G (EVs to power grid) represents EVs discharging energy back to the power grid for financial benefits. G2B (power grid to BESS) refers to the power grid charging the BESS, typically occurring during off-peak periods when the stored energy can be used later. Conversely, B2G (BESS to power grid) occurs during peak hours, where the BESS discharges excess energy to the power grid for economic returns. B2V (BESS to EVs) indicates that the BESS supplies power directly to EVs, commonly during peak periods, reducing their dependency on the power grid.

From the perspective of information flow, information from the power grid, EVs, and the BESS are aggregated in the EMS. After processing through optimization algorithms, the EMS generates charging and discharging schedules and transmits them back to the EVs and the BESS. Specifically, the EMS collects charging demand

information from EVs, including user preference, the expected SOC, the current SOC, and the parking duration at the charging station. Using this information as input parameters, the EMS determines the optimized charging and discharging schedule for each EV. Then, the EMS generates an optimized charging and discharging schedule for the BESS. Furthermore, we adopt a time-of-use electricity price, which is commonly used in real-world applications. Under this pricing model, electricity prices fluctuate across different time periods, such as peak and off-peak hours, and are known in advance for each time slot.

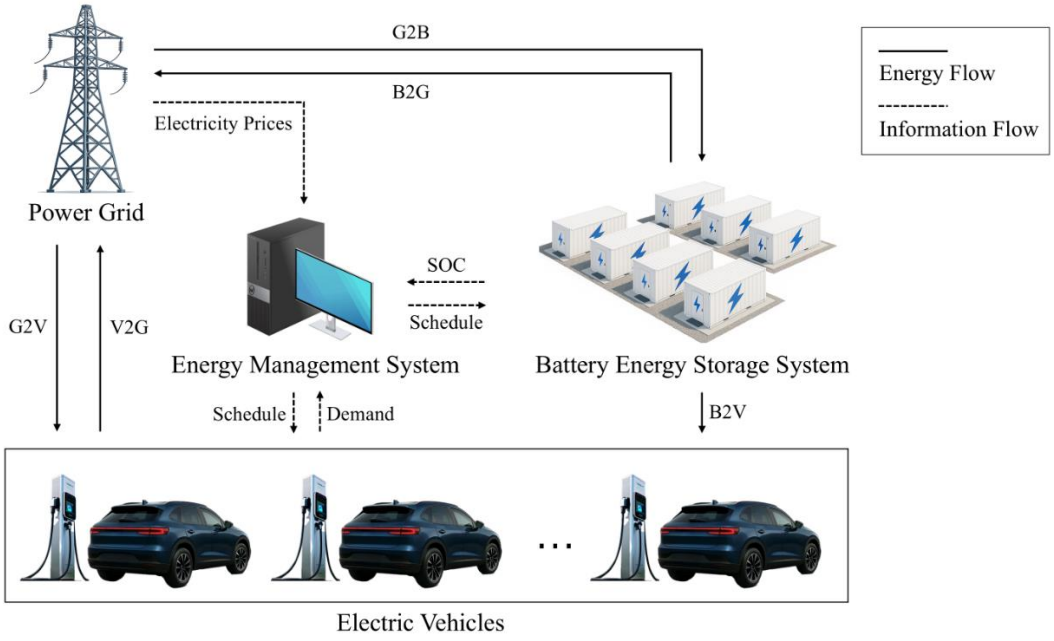

Figure 1 The architecture of the charging station

To provide a concrete visualization of the optimization results yielded by the UPEM problem, we present an illustrative example of daily operation schedules in Figure 2. The generated profiles illustrate the decision-making results over a 24-hour horizon. Figure 2(a) depicts the aggregated net power profile of the EVs, distinguishing between the total charging power and the V2G discharge power. Figure 2(b) displays the power scheduling of the BESS. Correspondingly, Figure 2(c) tracks the temporal evolution of the stored energy within the BESS. Notably, the maximum energy level observed in this curve is identified as the construction capacity for the BESS.

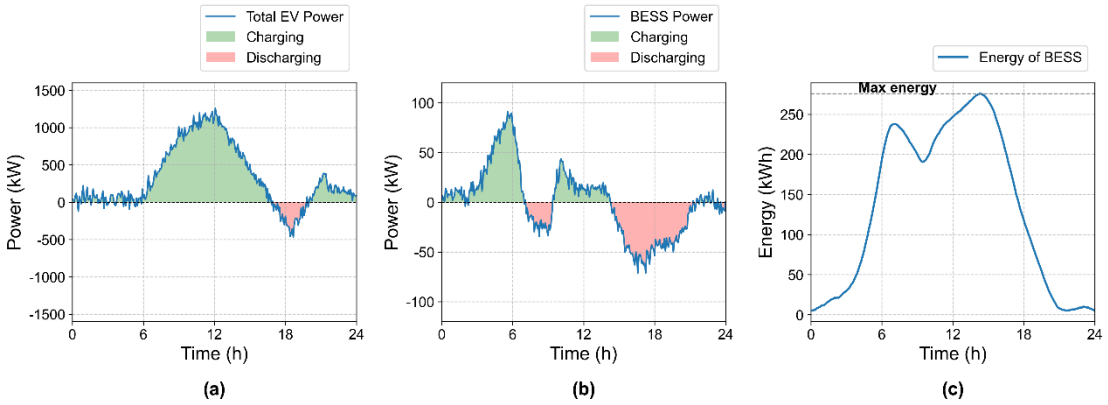

Figure 2 Illustrative example of daily operation scheduling for the UPEM problem

3.1 User preference

This study considers two types of user preferences: one of them is time-sensitive and requires charging at maximum power without intervention from the charging station. While the other is cost-sensitive and seeks to fulfill charging demands within a specified period, accepting power schedule and discharging to the power grid to reduce costs. Furthermore, the charging demand of cost-sensitive users is influenced by the current electricity price, increasing when the price is low and decreasing when it is high. This behavior is modeled using a fuzzy logic controller, as shown in Table . Specifically, the fuzzy logic controller adjusts the charging demand of cost-sensitive users based on two inputs: the current SOC of the EV and the electricity price. The SOC is fuzzified into five membership sets—very low, low, medium, high, and very high—using the membership function (Viegas & Da Costa, 2021) illustrated in Figure 3. Meanwhile, the electricity price follows a time-of-use structure with three levels: low, medium, and high. The output of the fuzzy logic controller represents the percentage change in the user's original charging demand. For example, if a user initially intends to charge 40% of the battery, and their SOC is "very low" while the electricity price is "low". Their charging demand will increase by 50% according to Table , resulting in a final demand of $40\% \times (1 + 50\%) = 60\%$.

Table 2 Fuzzy logic controller for charging demand change of price-sensitive users

SOC of EV	Electricity price		
	Low	Medium	High
Very low	+50%	+25%	0%
Low	+37.5%	+12.5%	-12.5%
Medium	+25%	0%	-25%
High	+12.5%	-12.5%	-37.5%
Very high	0%	-25%	-50%

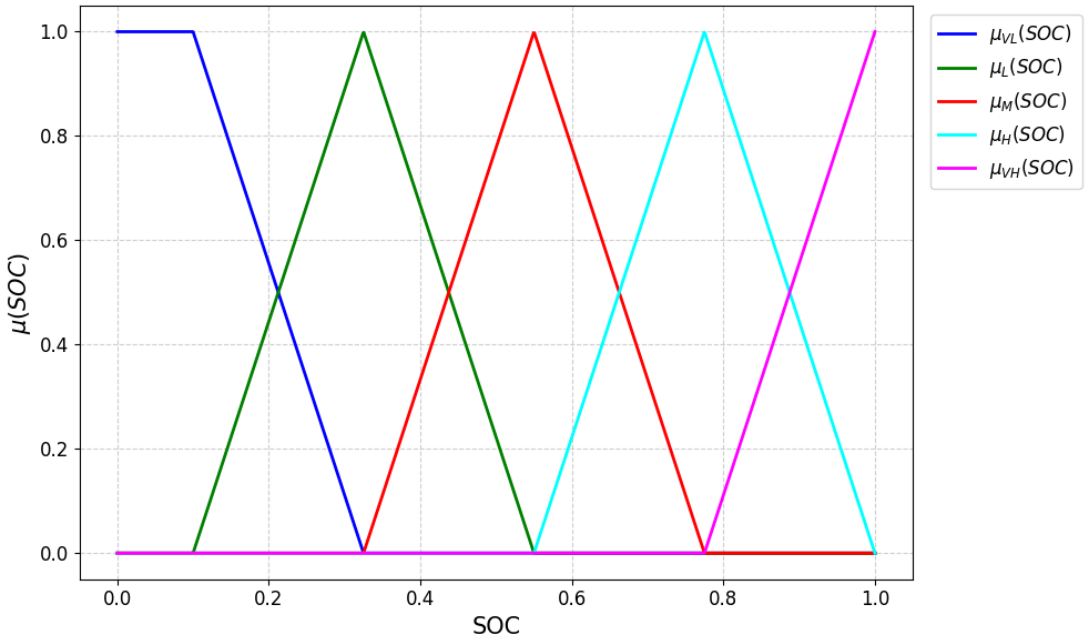

Figure 3 Membership functions of SOC for EVs

3.2 Objective function

This study focuses on minimizing operational costs while satisfying user demands by optimizing power allocation across different time periods. The notation used in the mathematical formulation is summarized in Table 3.

Table 3 Notation for definition of the model

Sets and parameters	
T	Set of discrete time periods, indexed by t

I	Set of electric vehicles (EVs), indexed by i
C_e	Electricity cost
C_b	BESS investment cost
C_p	Penalty cost associated with unmet charging demands of EV users
BCC	Capacity cost coefficient of BESS
BPC	Power cost coefficient of BESS
UPC	Unit penalty cost
DOD	Maximum depth of discharge of the EV battery
α	Proportion of the electricity price paid by the power grid as revenue for discharged energy.
η^{BESS}	Charging and discharging efficiency
EP_t	Electricity price during time period t
p_t^G	Power supplied from the power grid to the charging station during time period t
p_t^{B2G}	Power discharged from the BESS to the power grid during time period t
p_t^{B2E}	Power discharged from the BESS to the EV during time period t
E_t^{BESS}	Energy of BESS at the end of time period t
E_{max}^{BESS}	Maximum BESS capacity throughout the day
E_{min}^{BESS}	Minimum allowable energy of the BESS
p_t^{BESS}	BESS charging and discharging power during time period t
AG_t^{cyc}	Cycle degradation of the BESS during time period t
N_t^{fail}	Cycle life of the BESS from a fully charged state to the end of time period t
DE_i	Demand energy of EV i
E_{i,t_n}^{EV}	Actual energy of EV i at the end of charging
AT_i/DT_i	Arrival and departure times of EV i
IE_i	Initial energy of EV i
ME_i^{EV}	Maximum energy capacity of EV i

Decision variables

$p_{i,t}^{EV}$	Charging and discharging power of EV i during time period t
p_t^{BESS}	Charging and discharging power of the BESS during time period t
Auxiliary variables	
$CH_{i,t}^{EV}$	Binary variable indicating the charging status of EV i during time period t (1 for charging and 0 otherwise)
$DCH_{i,t}^{EV}$	Binary variable indicating the discharging status of EV i during time period t (1 for discharging and 0 otherwise)
CH_t^{BESS}	Binary variable indicating the charging status of the BESS during time period t (1 for charging and 0 otherwise)
DCH_t^{BESS}	Binary variable indicating the discharging status of the BESS during time period t (1 for discharging and 0 otherwise)

Accordingly, the objective function is designed to minimize total operational costs, which include electricity costs, BESS investment costs, and penalty costs, as formulated below:

$$Min\left(C_e + C_b + C_p\right) \tag{1}$$

The components of the objective function are defined as follows: First, the electricity cost (C_e) is calculated as the cost on purchasing electricity from the power grid minus the revenue from discharging to the power grid, as given by:

$$C_e = \sum_{t\in T}\left(p_t^G + \left(\sum_{i\in I} p_{i,t}^{EV}\cdot DCH_{i,t}^{EV}\cdot\alpha\right) - p_t^{B2G}\cdot\alpha\right)\cdot\Delta t\cdot EP_t \tag{2}$$

Let $T=\{t_0,t_1,t_2,\ldots,t_n\}$ denote the set of all discrete time periods, where t_0 represents a virtual time period introduced to define the initial state of the charging station at the onset of the scheduling process. Let I denote the set of all EVs. The index $t\in T$ represents a time period and $i\in I$ denotes an EV. The p_t^G represents the power input from the power grid to the charging station during time period t. The variable $p_{i,t}^{EV}$ represents the charging and discharging power of EV i during time period t, where a positive value indicates charging and a negative value indicates discharging.

The binary variable $DCH_{i,t}^{EV}$ takes a value of 1 if EV i is discharging during time period t and 0 otherwise. The term p_t^{B2G} represents the power discharged from the BESS to the power grid during time period t. The coefficient α ($\alpha \in (0,1]$) denotes the proportion of the electricity price at which the power grid pays as revenue for the energy discharged by the charging station. Hence, both EVs and the BESS receive revenue at a fraction α of the electricity price when discharging to the grid. The term Δt represents the length of a time period, and EP_t represents the electricity price during time period t.

Second, the BESS investment cost (C_b) refers to the allocation of its total investment over daily usage. Since the charging and discharging processes cause capacity degradation, and the BESS reaches its end-of-life when its capacity declines to 80% of the original value (Amini et al., 2023), the daily investment cost is determined based on this degradation. Specifically, it can be calculated by multiplying the total investment by the ratio of the BESS's capacity degradation in one day to the total allowable degradation. Additionally, the investment cost consists of capacity and power costs: the capacity cost covers the procurement of batteries with a specified energy limit, while the power cost includes the expenses associated with power electronics such as converters and transformers. The investment cost is formulated as follows:

$$C_b = \left(BCC \cdot E_{max}^{BESS} + BPC \cdot \max_{t \in T}(|p_t^{BESS}|)\right) \cdot \frac{\sum_{t \in T} AG_t^{cyc}}{0.2 \cdot E_{max}^{BESS}} \quad (3)$$

The term BCC denotes the capacity cost coefficient of BESS, representing the cost per unit of additional capacity. The term E_t^{BESS} refers to the energy of BESS at the end of time period t, while E_{max}^{BESS} captures the maximum BESS capacity throughout the day, yielding the total capacity cost $BCC \cdot E_{max}^{BESS}$. Similarly, BPC represents the power cost coefficient of BESS, indicating the cost per unit increase in maximum charging and discharging power. The term p_t^{BESS} denotes the BESS charging and discharging power during time period t, where positive values indicate charging and negative values indicate discharging. Taking the absolute value ensures a nonnegative maximum power value $\max_{t \in T}(|p_t^{BESS}|)$, leading to the total power cost $BPC \cdot \max_{t \in T}(|p_t^{BESS}|)$. The

fraction $\frac{\sum_{t\in T} AG_t^{cyc}}{0.2\cdot E_{max}^{BESS}}$ represents the inverse of the expected BESS lifetime, converting the total investment into a daily expense. Here, $\sum_{t\in T} AG_t^{cyc}$ denotes the total daily aging of the BESS, and $0.2 \cdot E_{max}^{BESS}$ corresponds to the maximum allowable capacity degradation over its lifespan.

Finally, the penalty cost (C_p) accounts for the penalty incurred for failing to meet users' charging demands. Instead of imposing a strict constraint on meeting charging demands, this cost introduces a soft constraint in the objective function, preventing excessive restrictions on the solution space and enhancing solution diversity. The penalty cost is computed as follow:

$$C_p = UPC \cdot \sum_{i\in I} max\left(0, DE_i - E_{i,t_n}^{EV}\right) \tag{4}$$

The term UPC represents the unit penalty cost. The term DE_i denotes the demand energy of EV i, and E_{i,t_n}^{EV} is the actual energy of EV i at the end of charging. The difference $DE_i - E_{i,t_n}^{EV}$ measures the gap between the demand and actual energy. Since some EVs may receive surplus energy, the function $max\left(0, DE_i - E_{i,t_n}^{EV}\right)$ function ensures that only unmet demands contribute to the penalty cost, providing an accurate representation of the penalty incurred.

3.3 Constraints

The decision variables in this study are $p_{i,t}^{EV}$ and p_t^{BESS}, representing the charging and discharging power of each EV and the BESS at each time period, respectively. The ranges of these decision variables are as follows:

$$p_{i,t}^{EV} \in [-p_{max}^{EV}, p_{max}^{EV}], \qquad \forall i, \forall t \tag{5}$$

$$p_t^{BESS} \in [-p_{max}^{BESS}, p_{max}^{BESS}], \qquad \forall t \tag{6}$$

A positive value of $p_{i,t}^{EV}$ or p_t^{BESS} indicates charging, while a negative value represents discharging.

3.3.1 Constraints of the BESS

- Initial and final energy of the BESS:

$$E_{t_0}^{BESS} = E_{t_n}^{BESS} = E_{min}^{BESS} \tag{7}$$

The initial and final energy of the BESS are set equal to prevent energy accumulation effects. Here, E_{min}^{BESS} is the minimum allowable energy of the BESS, a constant greater than zero to prevent over-discharge.

- Minimum energy constraint of the BESS:

$$E_t^{BESS} \geq E_{min}^{BESS}, \qquad \forall t \tag{8}$$

- Auxiliary variables indicating charging and discharging status of the BESS:

$$CH_t^{BESS} = \begin{cases} 0, & p_t^{BESS} \leq 0 \\ 1, & p_t^{BESS} > 0 \end{cases}, \qquad \forall i, \forall t \tag{9}$$

$$DCH_t^{BESS} = \begin{cases} 0, & p_t^{BESS} \geq 0 \\ 1, & p_t^{BESS} < 0 \end{cases}, \qquad \forall i, \forall t \tag{10}$$

Here, CH_t^{BESS} and DCH_t^{BESS} indicate whether the BESS is charging or discharging, respectively. The BESS can be in one of three states: charging, discharging, or idle, but it cannot charge and discharge simultaneously.

- Energy update of the BESS at the end of time period t:

$$E_t^{BESS} = E_{t-1}^{BESS} + \Delta t \cdot p_t^{BESS} \cdot \left(CH_t^{BESS} \cdot \eta^{BESS} + \frac{DCH_t^{BESS}}{\eta^{BESS}} \right), \qquad t \in [t_1, t_n] \tag{11}$$

This equation describes the change in BESS energy from the start to the end of time period t where η^{BESS} represents the charging and discharging efficiency.

- The cycle degradation of the BESS:

$$E_{max}^{BESS} = \max_{t \in T} (E_t^{BESS}) \tag{12}$$

$$N_t^{fail} = \left(\frac{20}{7.1568 \cdot \exp(0.02717 \cdot 298.15) \cdot \left(1 - \frac{E_t^{BESS}}{E_{max}^{BESS}}\right)^{0.4904} \cdot 10^{-4}} \right)^2, \quad \forall t \tag{13}$$

$$AG_t^{cyc} = \left(\frac{0.2 \cdot E_{max}^{BESS}}{N_t^{fail}} - \frac{0.2 \cdot E_{max}^{BESS}}{N_{t-1}^{fail}} \right) \cdot DCH_t^{BESS}, \qquad t \in [t_1, t_n] \tag{14}$$

We adopts the semi-empirical method proposed by Amini et al. (2023) to calculate the cycle degradation of the BESS. Battery degradation typically consists of calendar aging

and cycle aging. Calendar aging refers to the natural degradation process that occurs over time, while cycle aging refers to the capacity loss that occurs during the charge and discharge cycles of the battery. In this study, due to the short scheduling period of one day, the effect of calendar aging is negligible and can be ignored. Moreover, calendar aging is time-dependent and unrelated to the scheduling operations of the BESS, meaning that calendar degradation is identical across different schedules. Therefore, to simplify the calculation, only cycle aging is considered in the constraint conditions. Specifically, N_t^{fail} represents the cycle life of the BESS from a fully charged state to the end of time period t, and it is calculated using an empirical formula based on actual battery capacity degradation data. AG_t^{cyc} represents the cycle degradation of the BESS during time period t. The formula for calculating AG_t^{cyc} includes DCH_t^{BESS}, indicating that only the discharging periods need consideration. While cycle degradation encompasses both charging and discharging processes, the formula inherently incorporates the associated charging within the discharging calculations.

3.3.2 Constraints of EVs

- EV charging and discharging time limitation:

$$p_{i,t}^{EV} = 0, \qquad \forall t \notin [AT_i, DT_i] \tag{15}$$

An EV can only charge or discharge during its parking duration at the charging station, where AT_i and DT_i denote the arrival and departure times of EV i, respectively.

- Initial energy of EV:

$$E_{i,t_0}^{EV} = IE_i, \qquad \forall i \tag{16}$$

where IE_i represent the initial energy of EV i.

- EV energy bounds:

$$(1 - DOD) \cdot ME_i^{EV} \leq E_{i,t}^{EV} \leq ME_i^{EV}, \qquad \forall i, \forall t \tag{17}$$

where DOD is the maximum depth of discharge of the EV battery, and ME_i^{EV} is the maximum energy capacity of EV i.

- Auxiliary variables indicating charging and discharging status of EV:

$$CH_{i,t}^{EV} = \begin{cases} 0, & p_{i,t}^{EV} \le 0 \\ 1, & p_{i,t}^{EV} > 0 \end{cases}, \qquad \forall i, \forall t \tag{18}$$

$$DCH_{i,t}^{EV} = \begin{cases} 0, & p_{i,t}^{EV} \ge 0 \\ 1, & p_{i,t}^{EV} < 0 \end{cases}, \qquad \forall i, \forall t \tag{19}$$

Here, $CH_{i,t}^{EV}$ and $DCH_{i,t}^{EV}$ indicate whether the EV i is charging or discharging during time period t. Each EV can only be in one of three states: charging, discharging, or idle, and it cannot charge and discharge simultaneously.

- Energy update of EV at the end of time period t:

$$E_{i,t}^{EV} = E_{i,t-1}^{EV} + \Delta t \cdot p_{i,t}^{EV} \cdot \left(CH_{i,t}^{EV} \cdot \eta^{EV} + \frac{DCH_{i,t}^{EV}}{\eta^{EV}} \right), \qquad \forall i, t \in [t_1, t_n] \tag{20}$$

3.3.3 Constraints of power flow

- BESS-to-EV power transfer during time period t:

$$p_t^{B2E} = min\left(\sum_{i \in I} p_{i,t}^{EV} \cdot CH_{i,t}^{EV}, -p_t^{BESS} \cdot DCH_t^{BESS} \right), \qquad \forall t \tag{21}$$

The term $\sum_{i \in I} p_{i,t}^{EV} \cdot CH_{i,t}^{EV}$ represents the total charging power required by EVs, while $-p_t^{BESS} \cdot DCH_t^{BESS}$ represents the total discharging power of the BESS. If the BESS provides more power than the total EV demand, all EVs can be powered by the BESS alone; otherwise, the remaining demand must be met by the power grid.

- BESS-to-Grid power transfer during time period t:

$$p_t^{B2G} = -p_t^{BESS} \cdot DCH_t^{BESS} - p_t^{B2E}, \qquad \forall t \tag{22}$$

If there is surplus power after the BESS supplies the EVs, it is injected into the power grid for revenue generation.

- Power balance constraint at the charging station:

$$\left(\sum_{i \in I} p_{i,t}^{EV} \cdot CH_{i,t}^{EV} \right) + p_t^{BESS} \cdot CH_t^{BESS} = p_t^{G} + p_t^{B2E}, \qquad \forall t \tag{23}$$

The total power demand at the charging station equals the power supplied by the power grid and the BESS. Where p_t^G represents the overall power input from the power grid to the charging station, including the sum of the power released to the EVs and the BESS.

- Power limits at the power grid connection point:

$$0 \le p_t^G \le p_{max}^G, \qquad \forall t \tag{24}$$

$$0 \le p_t^{B2G} - \sum_{i \in I} \left(p_{i,t}^{EV} \cdot DCH_{i,t}^{EV} \right) \le p_{max}^G, \qquad \forall t \tag{25}$$

Both the power supplied by the power grid and the power injected into the power grid from the charging station must not exceed the maximum capacity of the power grid connection (p_{max}^G).

4. Solution approach

4.1 Algorithm framework

We adopt a rolling horizon approach to address the UPEM problem, as shown in Figure 4. This approach decomposes the dynamic scheduling problem into a series of static subproblems along the time dimension. We then solve these subproblems sequentially to gradually approximate the optimal solution of the main problem. Each static subproblem considers only the current state of the charging station, such as the number of EVs, their SOCs, the SOC of the BESS and so on. The objective is to determine the optimal capacity of the BESS and the charging and discharging powers for both the BESS and each EV. To solve the decomposed static subproblems, we propose a hybrid metaheuristic algorithm that comprises a greedy algorithm and a PSO algorithm. Specifically, we determine the power of EVs for each time period using the greedy algorithm based on their energy demand, parking duration, and electricity prices. For the BESS, given the EVs' charging and discharging power schedules, we employ the PSO algorithm to determine its power schedule for the rest of the day. The choice of PSO is motivated by the characteristics of the BESS scheduling subproblem. The charging and discharging power of the BESS is continuous over multiple time periods, resulting in a high-dimensional continuous search space. PSO is particularly well suited to continuous optimization and can directly search the BESS power schedules without requiring gradient information, which is advantageous for the simulation-based objective evaluation considered in this study. Moreover, the particle representation

naturally corresponds to the time-dependent BESS power decisions, allowing a straightforward solution encoding. These characteristics make PSO well suited to the BESS scheduling subproblem considered in this study.

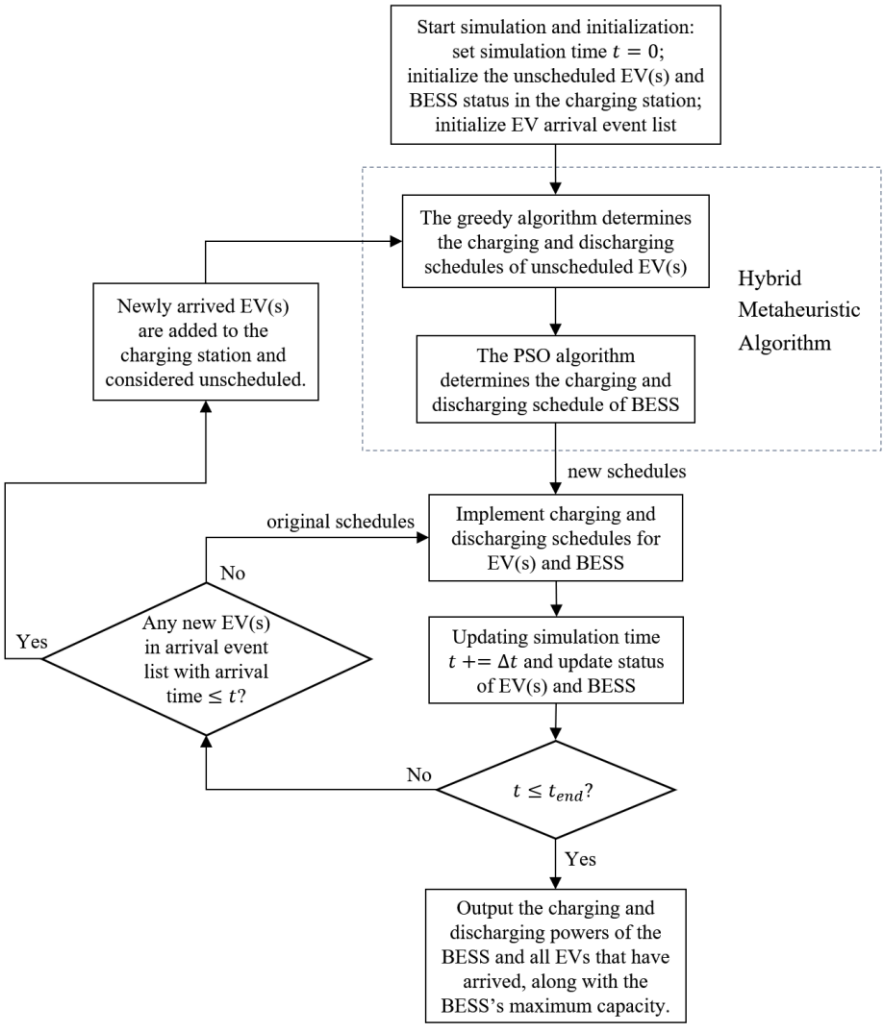

Figure 4 Algorithm framework

A detailed explanation of the algorithm framework is provided as follow. Initially, we set the simulation time $t = 0$ and initialize the state of the charging station. The initialization includes setting the BESS energy to its minimum value and establishing several unscheduled EVs with their current SOC, charging requirements, and departure times. Specifically, unscheduled EVs refer to those without designated charging and discharging schedules. Furthermore, an EV arrival event list needs to be initialized, comprising each EV's arrival time, SOC, charging demand, and other relevant states.

Once initialized, the iteration begins with a greedy algorithm employing to develop charging and discharging schedules for each unscheduled EV. Subsequently, considering the charging and discharging schedules of all EVs, the PSO algorithm is used to develop a charging and discharging schedule for the BESS. Once all schedules are determined, the corresponding schedule for the current time period is executed. After that, the simulation time is updated to $t = t + \Delta t$, and the energy states of the EVs and BESS are synchronously updated. And EVs are removed from the charging station if they have reached their departure time. Subsequently, it is evaluated whether any new EVs have arrived between $t - \Delta t$ and t based on the EV arrival event list. If arrivals occur, they are moved into the charging station and marked as unscheduled. The process then proceeds to the next iteration until the termination time t_{end} is reached, at which point the algorithm concludes. Upon completion, the algorithm outputs the charging and discharging powers of the BESS and all EVs at different time periods, and the maximum capacity of the BESS is also provided as its optimal capacity.

4.2 Greedy algorithm

To develop charging and discharging schedules for EVs, we refer to the heuristic method proposed by Cao et al. (2012) and incorporate the V2G characteristics of the UPEM problem. Based on this, we design a greedy algorithm to determine the charging and discharging powers of EVs across different time slots, as illustrated in Algorithm 1. This greedy algorithm sequentially determines the charging and discharging schedule for each EV during its parking duration. Each run of the algorithm focuses on a single EV, and repeating the algorithm for all EVs yields the charging and discharging schedules for all EVs. The greedy algorithm operates as follows: First, it sorts all time slots in ascending order of electricity price. When multiple time slots have the same electricity price, they are further ordered chronologically (line 1). Then, an initial charging schedule is generated, where the EV charges at its maximum allowable power until its charging demand is satisfied (line 3). Subsequently, the SOC at the end of each time slot is calculated (line 4), which helps check whether energy limit constraints are violated in subsequent steps. The next stage involves allocating discharging power. In

this stage, discharging power is increased during high-price time slots (denoted as ts_i), while charging power is simultaneously increased during low-price time slots (denoted as ts_j), ensuring that the EV's SOC still satisfies its charging demand. The last time slot ts_n is selected as the initial discharging slot, and the first time slot ts_1 is selected as the initial charging slot (line 6). The algorithm then checks whether more charging or discharging power can be increased in ts_i and ts_j (line 8, line 9). If the conditions are met, a fixed amount of power p will be added to the discharging power at ts_i and to the charging power at ts_j (line 10). After updating the power values, the SOC in the end of each time slot must also be updated to ensure that the EV's SOC remains within the feasible bounds (line 11). If the power adjustment causes any energy limits constraint to be violated, the charging and discharging powers roll back to the state before adjustment (line 13). The algorithm then continues to optimize the power allocation for other time slots (line 16, line 19), until no further improvement is possible. Finally, the algorithm terminates and outputs the optimized charging and discharging schedule for the EV (line 22).

Algorithm 1 Greedy algorithm for EV charging and discharging scheduling

Input: demand energy DE, maximum charging and discharging power P_{max}, time slots $T = \{t_1, t_2, \ldots, t_n\}$, time slot length Δt, power transfer step p, electricity prices $EP(t_i)$

Output: optimized power schedule for EV $P(t_i)$

1: $TS \leftarrow Sort(T)$ ▷ Sort time slots by electricity price, then by time if equal
2: **for** $i \leftarrow 1$ to n **do**
3: $P(ts_i) = min(P_{max}, (DE - E)/\Delta t)$ ▷ Charge the EV at maximum power until the demand is met
4: $E(ts_i) = E(ts_{i-1}) + P(ts_i) * \Delta t$ ▷ Calculate the energy of EV at the end of each time slot
5: **end for**
6: $i \leftarrow n$; $j \leftarrow 1$ ▷ ts_i: discharging power increase period, ts_j: charging power increase period
7: **while** $EP(ts_i) > EP(ts_j)$ **do**
8: **if** $P(ts_i) - p \geq -P_{max}$ **then** ▷ Check if ts_i can increase discharging power
9: **if** $P(ts_j) + p \leq P_{max}$ **then** ▷ Check if ts_j can increase charging power
10: $P(ts_i) \leftarrow P(ts_i) - p$; $P(ts_j) \leftarrow P(ts_j) + p$ ▷ Update schedule
11: Recalculate $E(ts_k)$ for all time slots.

12: **if** $E(ts_k) < 0 \; or \; E(ts_k) > E_{max}, \exists k$ **then** ▷ Check schedule feasibility and roll back if infeasible
13: $P(ts_i) \leftarrow P(ts_i) + p;\ P(ts_j) \leftarrow P(ts_j) - p$
14: **end if**
15: **else**
16: $j \leftarrow j + 1$
17: **end if**
18: **else**
19: $i \leftarrow i - 1$
20: **end if**
21: **end while**
22: **return** $P(t_i)$ ▷ Returns optimized power schedule for EV

4.3 Particle swarm optimization algorithm

In the PSO algorithm, each solution is represented as a vector where each dimension corresponds to a specific time slot, and the value indicates the power of the BESS in that time slot. The overall procedure, illustrated in Algorithm 2, consists of initialization, fitness evaluation, particle update, and termination condition checking. First, the particle swarm is initialized. The position and velocity of each particle are randomly assigned within the search space (line 2). Simultaneously, each particle's personal best position is initialized to its current position (line 3). To improve the initial solution quality, we also introduce a rule-based particle into the initial swarm (line 5). Specifically, for each value (denoted as x_s^t) at dimension t of the rule-based particle position x_s, the rule checks the electricity price at time slot t and assigns the corresponding power. If the electricity price at time slot t is higher than the prices in all subsequent time slots, then x_s^t is set to $-p_{max}^{BESS}$; if the electricity price at time slot t is the lowest among all time slots, then x_s^t is set to p_{max}^{BESS}; otherwise, x_s^t is set to 0. Next, the fitness of each particle (i.e., the objective function value) is evaluated (line 7), and the global best position is updated accordingly (line 8). Additionally, if a particle's current fitness exceeds its personal best, the particle's best position is updated. Likewise, if a particle's fitness surpasses the global best fitness, the global best position is updated as well. The inertia weight ω is then updated (line 9). This weight controls the influence of a particle's previous velocity on its current velocity. We adopt a linear-

varying inertia weight (LVIW) technique (Shi & Eberhart, 1999), where ω linearly decreases from its initial value ω_s to the final value ω_e over iterations. This technique encourages broader exploration in early iterations and more focused exploitation in later stages, thereby improving the overall algorithm performance (Shami et al., 2022). Following the fitness evaluation, the velocity of each particle is updated using the following formula (line 12):

$$v_{j+1,k} = \omega \cdot v_{j,k} + c_1 \cdot r_1 \cdot \left(p_k - x_{j,k}\right) + c_2 \cdot r_2 \cdot \left(g - x_{j,k}\right) \tag{26}$$

Here, $v_{j,k}$ denotes the velocity of particle k at iteration j. The constants c_1 and c_2 are acceleration coefficients that guide the particle towards its personal best position p_k and the global best position g, respectively. r_1 and r_2 are random values within $[0,1]$. The particle's position is then updated as follows (line 13):

$$x_{j+1,k} = x_{j,k} + v_{j+1,k} \tag{27}$$

After updating particle positions, we apply an optimization rule to eliminate dominated solutions and enhance solution quality. Specifically, for each particle, we check the following two conditions in every time slot (line 15): (1) The BESS is charging in the current time slot, and no subsequent time slot has a higher electricity price. (2) The BESS is discharging in the current time slot, and this slot has the lowest electricity price among all. If either condition is satisfied, the charging or discharging power in the corresponding time slot is reset to 0 (line 16). The rationale is as follows: for condition (1), if there are no higher-price slots ahead, charging will not be profitable through price arbitrage, but will instead incur unnecessary cost. For condition (2), discharging during the lowest-price slot is unprofitable, thus making the operation economically inefficient. This optimization rule aims to eliminate dominated solutions and avoid ineffective or even detrimental operations, thereby improving the rationality and efficiency of the solutions. Finally, if the maximum number of iterations is reached, the algorithm terminates and outputs the global best solution (line 21). Otherwise, the process continues to the next iteration.

Algorithm 2 PSO algorithm for BESS charging and discharging scheduling

Input: dimensions of particles n, population size s, maximum iterations j_{max},

inertia weight range $[\omega_s, \omega_e]$, acceleration coefficients c_1, c_2, electricity prices $EP\ (t_i)$

Output: optimized power schedule g

for $k \leftarrow 2$ to s **do**
  $x_{1,k}, v_{1,k} \leftarrow initParticle(\ )$ ▷ Initialize particle positions $x_{1,k}$ and velocities $v_{1,k}$ randomly within feasible range
  $p_k \leftarrow x_{1,k}$ ▷ Initialize particle's personal best position p_k
end for
$x_{1,1}, v_{1,1}, p_1 \leftarrow ruleParticle(\ )$ ▷ Generate particle using empirical rule
for $j \leftarrow 1$ to j_{max} **do**
  $F_j \leftarrow evaluateFitness(x_j)$ ▷ Evaluate fitness for all particles
  $g \leftarrow getBest(x_j, F_j)$ ▷ Update the global optimal position
  $\omega \leftarrow \omega_s - j \times (\omega_s - \omega_e)/j_{max}$ ▷ Update inertia weight
  for $k \leftarrow 1$ to s **do**
    $r_1, r_2 \leftarrow random(\ )$ ▷ Generate random numbers $r_1, r_2 \in [0, 1]$
    $v_{j+1,k} \leftarrow \omega \cdot v_{j,k} + c_1 \cdot r_1 \cdot (p_j - x_{j,k}) + c_2 \cdot r_2 \cdot (g - x_{j,k})$ ▷ Update velocity
    $x_{j+1,k} \leftarrow x_{j,k} + v_{j+1,k}$ ▷ Update position
    for $i \leftarrow 1$ to n **do**
      if $(x_{j+1,k}[i] > 0\ and\ \nexists\ EP\ (t_m) > EP\ (t_i), m > i)$ **or** $(x_{j+1,k}[i] < 0\ and\ \nexists\ EP\ (t_m) < EP\ (t_i), m \neq i)$ **then**
        $x_{j+1,k}[i] \leftarrow 0$ ▷ Modify the dominated particle based on the optimization rule
      end if
    end for
  end for
end for
return g ▷ Returns optimized power schedule for BESS

5. Experimental research

This section presents a series of computational experiments to comprehensively evaluate the performance of the proposed approach. The proposed algorithm was developed and implemented in C++. All computational experiments were performed on a server cluster, with each computing node equipped with dual Intel® Xeon® Gold 6226R processors and 256 GB of RAM.

5.1 Parameter settings

To address the dynamic nature of the UPEM problem, we discretize it into multiple static subproblems using a fixed time interval. Considering that the granularity of this

discretization directly affects algorithm efficiency, the time interval Δt is set to 5 minutes to strike a balance between responsiveness and computational efficiency. The charging station considered in this study is equipped with 25 identical charging piles. We adopt time-of-use electricity price data from Guangdong Province, China. Specifically, the peak period is from 10:00 to 12:00 and 14:00 to 19:00, during which the electricity price is 1.0377 Yuan/kWh. The off-peak period is from 00:00 to 08:00, with a price of 0.2320 Yuan/kWh. All other hours are classified as flat periods, with a price of 0.6104 Yuan/kWh. When discharging to the grid, EVs and BESS receive an economic return based on a fixed proportion (α) of electricity price, which is set to 0.8. A penalty cost is incurred if the user's charging demand is not fully met, with the unit penalty cost (UPC) set at 2.0754 Yuan/kWh—twice the maximum electricity price—which is sufficiently high to ensure that user demand is fulfilled. Users are split 40% time-sensitive and 60% price-sensitive. Furthermore, we adopt EV and BESS-related parameters from Han (Han, 2024). To ensure the simulation data closely reflects real-world conditions, the top five best-selling EVs in China from 2023 to 2024 were selected as the basis for simulation data. The battery capacity, maximum charging and discharging power, depth-of-discharge (DOD) and charging and discharging efficiency were calculated as weighted averages based on their respective sales volumes. For computational simplicity, the results were approximated. Specifically, the EV battery capacity is 50 kWh, with a maximum charging and discharging power of 60 kW, a DOD of 0.9, and a charging and discharging efficiency of 0.9. Parameters for the BESS are provided in Table . Among them, the maximum charging and discharging power and the minimum capacity are customized according to the characteristics of the UPEM problem. The power cost coefficient in the table represents the cost incurred for each 1 kW increase in maximum power, primarily reflecting the construction cost of components such as converters and transformers. The capacity cost coefficient represents the cost for each 1 kWh increase in maximum capacity.

Table 4 Parameter settings of BESS

Parameter	Value	Unit

BESS power cost coefficient（BPC）	2700	Yuan/kW
BESS capacity cost coefficient（BCC）	640	Yuan/kWh
Charging and discharging efficiency	0.80	/
Max charging and discharging power	100	kW
Minimum capacity of BESS	5	kWh

The parameter settings of the PSO algorithm are presented in Table . The parameter values were determined based on Juneja et al. (2016), and each parameter was individually tuned within a reasonable range.

Table 5 Parameter settings of the PSO algorithm

Parameter	Value
Start value of inertia weight (ω_s)	0.9
End value of inertia weight (ω_e)	0.3
Personal acceleration coefficient (c_1)	2
Social acceleration coefficient (c_2)	2
Population size	60
Maximum number of generations	300
Maximum iteration seconds	10

5.2 Experimental scenarios

We construct the charging and discharging demand of EVs based on Li et al. (2020). Specifically, the arrival time of users follows a two-parameter Weibull distribution with parameters $a = 0.9831$ and $b = 16.8$. The departure time follows a normal distribution with a mean of 18:00 and a standard deviation of 3. The initial SOC of EVs is normally distributed with a mean of 0.36 and a standard deviation of 0.15, while the demand SOC follows a normal distribution with a mean of 0.86 and a standard deviation of 0.14. Based on these distributions, we design a series of scenarios with varying number of EV users and average parking durations to evaluate the performance of the hybrid metaheuristic algorithm under different conditions. First, we define a

baseline scenario with a small number of users and medium parking durations (SU-MD scenario), where 50 EVs arrive throughout the day, and the average departure time is 18:00. To examine the impact of the number of users, we further construct medium number of users (MU-MD scenario) and large number of users (LU-MD scenario) scenarios by setting the number of users to 75 and 100, respectively, while keeping all other parameters unchanged. We also explore how variations in average parking duration influence charging and discharging demand. Specifically, the user's parking duration is determined by their arrival and departure times. To simplify the scenario generation process, we fix the distribution parameters of arrival times and adjust only the mean of the departure time distribution when varying the average parking duration. Building on the SU-MD scenario, we set the average departure time to 17:00 and 19:00, respectively, to construct a short-duration (SU-SD scenario) and a long-duration (SU-LD scenario) parking scenarios, with all other parameters held constant. These departure times were selected to reflect peak end-of-work hours, enabling us to study the impact of different average parking durations.

5.3 Results and analysis

5.3.1 Comparison between Gurobi and the greedy algorithm

To validate the proposed mathematical formulation and evaluate the solution quality of the greedy algorithm, we employed the commercial optimization solver Gurobi as an exact benchmark. The experiments were conducted using Gurobi Optimizer 9.0.3. Specifically, the EV-level scheduling subproblem was extracted from the overall formulation and solved independently by Gurobi. This subproblem aims to minimize the electricity cost of an individual EV while satisfying its charging/discharging power limits and battery energy constraints. A test instance containing 50 EVs was generated according to the settings of the SU-MD scenario. For each EV, Gurobi and the greedy algorithm were applied under identical problem settings, and the obtained objective values and corresponding gaps are reported in Table 6. Both methods were able to solve all EV-level scheduling problems within 10 s.

As shown in Table 6, Gurobi successfully obtained proven optimal solutions for

all 50 single-EV scheduling problems. This result supports the validity and solvability of the EV-level formulation derived from the proposed mathematical model, demonstrating that the charging and discharging decisions and associated constraints can be effectively handled by a commercial optimization solver. Moreover, the greedy algorithm achieved the same objective value as Gurobi for every EV, resulting in a gap of 0% in all cases. These results demonstrate that the proposed greedy algorithm can effectively high-quality optimal solutions for the tested single-EV scheduling problems. Therefore, the greedy algorithm provides an effective approach for determining EV charging and discharging schedules and can be efficiently integrated into the proposed rolling horizon solution framework.

Table 6 Comparison between Gurobi and the greedy algorithm for single-EV scheduling problems

EV	Gurobi	Greedy	Gap (%)	EV	Gurobi	Greedy	Gap (%)
1	-7.34	-7.34	0.00	26	1.69	1.69	0.00
2	0.68	0.68	0.00	27	18.70	18.70	0.00
3	7.36	7.36	0.00	28	-7.55	-7.55	0.00
4	4.61	4.61	0.00	29	-2.38	-2.38	0.00
5	-13.52	-13.52	0.00	30	23.69	23.69	0.00
6	-6.72	-6.72	0.00	31	9.58	9.58	0.00
7	9.86	9.86	0.00	32	-6.38	-6.38	0.00
8	18.10	18.10	0.00	33	6.36	6.36	0.00
9	-5.99	-5.99	0.00	34	-12.43	-12.43	0.00
10	8.06	8.06	0.00	35	13.62	13.62	0.00
11	1.72	1.72	0.00	36	5.07	5.07	0.00
12	17.26	17.26	0.00	37	-7.15	-7.15	0.00
13	4.69	4.69	0.00	38	10.02	10.02	0.00
14	1.41	1.41	0.00	39	-10.94	-10.94	0.00
15	-3.48	-3.48	0.00	40	-7.82	-7.82	0.00
16	9.99	9.99	0.00	41	7.86	7.86	0.00
17	23.56	23.56	0.00	42	20.61	20.61	0.00
18	-23.54	-23.54	0.00	43	6.28	6.28	0.00
19	15.17	15.17	0.00	44	-4.28	-4.28	0.00
20	0.00	0.00	0.00	45	-6.38	-6.38	0.00
21	-10.29	-10.29	0.00	46	-10.27	-10.27	0.00
22	1.03	1.03	0.00	47	-2.06	-2.06	0.00
23	-5.72	-5.72	0.00	48	32.05	32.05	0.00
24	1.07	1.07	0.00	49	0.48	0.48	0.00
25	-2.81	-2.81	0.00	50	4.08	4.08	0.00

5.3.2 Effectiveness experiment of V2G and BESS

To further evaluate the impact of incorporating V2G technology and BESS on the operational cost of the charging station, we compared the objective function values

under different configurations. We first conducted experiments to assess the effectiveness of V2G. Specifically, we compared the performance of our proposed V2G-integrated greedy algorithm and the non-V2G heuristic algorithm proposed by Cao et al. (2012), both of which do not employ BESS. These experiments were conducted across the five previously defined scenarios. For each scenario, 10 instances were generated based on the defined distribution to mitigate the influence of randomness. The experimental results are presented in Table and Figure 5. Additionally, we conduct a paired Wilcoxon signed-rank test comparing the heuristic algorithm and the greedy algorithm in each scenario, and the exact p-value is all 0.00195, indicating a highly significant difference. The results show that the greedy algorithm consistently outperforms the heuristic algorithm, achieving an average reduction of 22.91% in operational costs. This demonstrates that the V2G technology significantly improves the economic performance of the charging station. Notably, the SU-LD scenario achieves the highest V2G benefit, with an average cost reduction of 32.89%. This is because the longer parking durations provide more time for EV discharging once its charging demands are met.

Table 7 Experimental analysis of V2G effectiveness

Instance	Heuristic algorithm by Cao et al. (2012)	Greedy algorithm	Improvement over heuristic algorithm (%)
SU-MD-1	401.20	309.02	22.97
SU-MD-2	411.80	353.94	14.05
SU-MD-3	443.23	311.73	29.67
SU-MD-4	259.58	172.35	33.61
SU-MD-5	362.51	309.14	14.72
SU-MD-6	359.05	266.79	25.69
SU-MD-7	229.86	118.08	48.63
SU-MD-8	410.33	377.83	7.92
SU-MD-9	433.51	338.58	21.90
SU-MD-10	407.38	358.72	11.95
MU-MD-1	463.92	336.97	27.36
MU-MD-2	520.42	431.00	17.18
MU-MD-3	468.62	395.64	15.57
MU-MD-4	446.23	354.04	20.66
MU-MD-5	395.75	276.22	30.20
MU-MD-6	398.66	316.38	20.64
MU-MD-7	457.58	332.60	27.31
MU-MD-8	434.94	364.50	16.20
MU-MD-9	471.05	385.92	18.07
MU-MD-10	531.38	438.14	17.55

LU-MD-1	397.03	322.53	18.77
LU-MD-2	524.03	397.58	24.13
LU-MD-3	612.76	487.81	20.39
LU-MD-4	569.45	512.32	10.03
LU-MD-5	503.15	469.57	6.67
LU-MD-6	648.68	531.74	18.03
LU-MD-7	571.11	521.50	8.69
LU-MD-8	680.70	554.46	18.54
LU-MD-9	375.62	210.16	44.05
LU-MD-10	415.08	309.06	25.54
SU-SD-1	320.13	285.29	10.88
SU-SD-2	382.17	306.94	19.69
SU-SD-3	374.52	293.56	21.62
SU-SD-4	370.03	292.28	21.01
SU-SD-5	382.70	304.45	20.45
SU-SD-6	375.32	313.37	16.51
SU-SD-7	399.66	298.64	25.28
SU-SD-8	358.74	239.03	33.37
SU-SD-9	566.34	482.68	14.77
SU-SD-10	316.09	232.13	26.56
SU-LD-1	243.23	68.08	72.01
SU-LD-2	347.03	285.44	17.75
SU-LD-3	277.61	177.31	36.13
SU-LD-4	283.95	163.89	42.28
SU-LD-5	306.67	167.96	45.23
SU-LD-6	393.76	278.02	29.39
SU-LD-7	367.30	264.36	28.03
SU-LD-8	344.63	275.73	19.99
SU-LD-9	294.87	155.39	47.30
SU-LD-10	425.88	368.24	13.53

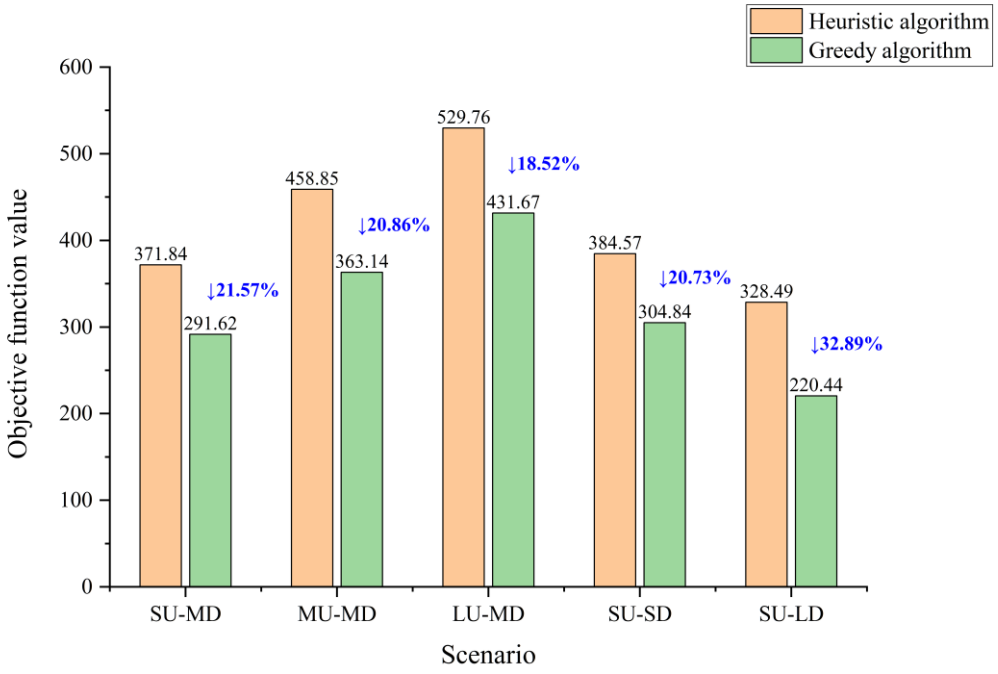

Figure 5 Average performance of heuristic algorithm and greedy algorithm

Next, we assessed the effectiveness of BESS by comparing the greedy algorithm without BESS to the hybrid metaheuristic algorithm with BESS. The results are shown in Table and Figure 6. Across all scenarios, a paired Wilcoxon signed-rank test between the greedy algorithm and the hybrid metaheuristic yields an exact p-value of 0.00195, underscoring a highly significant difference. The results reveal that the hybrid metaheuristic algorithm reduces operational costs by an average of 17.71%. This indicates that the economic performance of the charging station is significantly improved through the integration of BESS. Moreover, the SU-LD scenario achieved the greatest cost reduction by an average of 23.16%. This is because, in the SU-LD scenario, the extended parking duration of EVs reduces the number of users accessing the charging station, thereby reducing the overall charging demand. As a result, after meeting the charging demand of the EVs, the BESS can discharge more energy to the grid, further lowering costs.

Table 8 Experimental analysis of BESS effectiveness

Instance	Greedy algorithm	Hybrid metaheuristic		Average improvement over greedy algorithm (%)
		Average	Best	
SU-MD-1	309.02	261.45	260.80	15.39
SU-MD-2	353.94	297.58	297.58	15.92
SU-MD-3	311.73	259.37	259.37	16.80
SU-MD-4	172.35	128.11	128.11	25.67
SU-MD-5	309.14	259.07	259.07	16.20
SU-MD-6	266.79	213.85	213.85	19.85
SU-MD-7	118.08	71.35	71.35	39.57
SU-MD-8	377.83	315.78	315.78	16.42
SU-MD-9	338.58	275.83	275.83	18.53
SU-MD-10	358.72	306.55	306.55	14.54
MU-MD-1	336.97	282.30	280.77	16.23
MU-MD-2	431.00	371.93	371.93	13.71
MU-MD-3	395.64	330.22	328.83	16.54
MU-MD-4	354.04	301.40	301.20	14.87
MU-MD-5	276.22	222.44	222.44	19.47
MU-MD-6	316.38	248.16	248.00	21.56
MU-MD-7	332.60	281.21	279.49	15.45
MU-MD-8	364.50	307.23	307.23	15.71
MU-MD-9	385.92	326.63	326.09	15.36
MU-MD-10	438.14	373.64	373.64	14.72
LU-MD-1	322.53	277.43	277.43	13.98
LU-MD-2	397.58	332.04	332.04	16.48
LU-MD-3	487.81	419.01	416.58	14.10
LU-MD-4	512.32	444.32	444.12	13.27
LU-MD-5	469.57	415.13	411.69	11.59
LU-MD-6	531.74	470.25	470.25	11.56

LU-MD-7	521.50	463.58	463.58	11.11
LU-MD-8	554.46	492.11	491.20	11.25
LU-MD-9	210.16	160.81	160.81	23.48
LU-MD-10	309.06	258.52	258.15	16.35
SU-SD-1	285.29	236.56	236.03	17.08
SU-SD-2	306.94	249.31	246.96	18.78
SU-SD-3	293.56	239.01	239.01	18.58
SU-SD-4	292.28	228.49	228.49	21.83
SU-SD-5	304.45	250.33	250.33	17.78
SU-SD-6	313.37	268.37	267.81	14.36
SU-SD-7	298.64	247.96	247.96	16.97
SU-SD-8	239.03	194.18	194.18	18.76
SU-SD-9	482.68	409.82	409.82	15.09
SU-SD-10	232.13	185.97	185.97	19.89
SU-LD-1	68.08	24.68	24.68	63.75
SU-LD-2	285.44	236.16	236.16	17.26
SU-LD-3	177.31	130.05	130.05	26.65
SU-LD-4	163.89	114.91	114.91	29.88
SU-LD-5	167.96	117.29	117.29	30.17
SU-LD-6	278.02	217.43	217.43	21.79
SU-LD-7	264.36	202.65	202.65	23.34
SU-LD-8	275.73	229.49	227.09	16.77
SU-LD-9	155.39	108.30	107.00	30.31
SU-LD-10	368.24	313.01	313.01	15.00

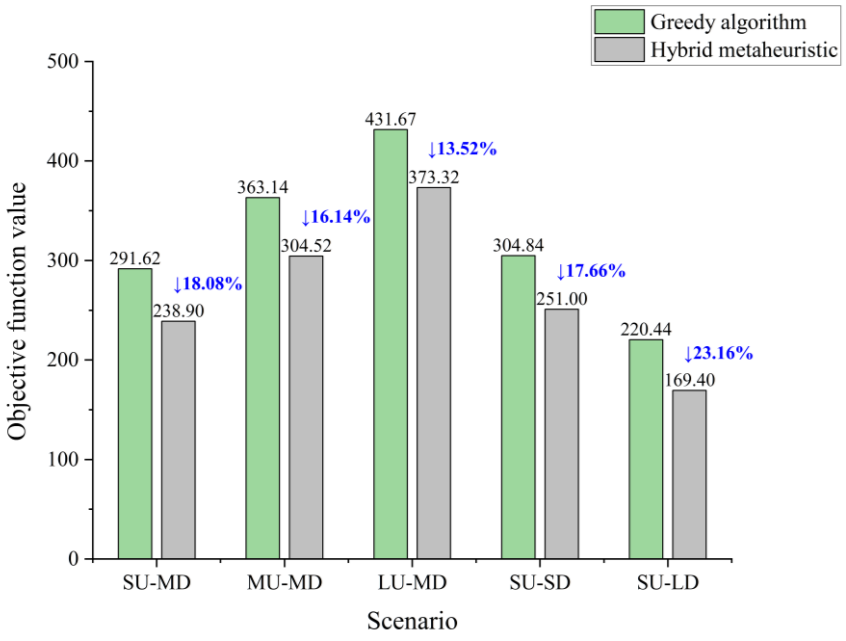

Figure 6 Average performance of greedy algorithm and hybrid metaheuristic algorithm

5.3.3 Performance comparisons among different scenarios

To evaluate the effectiveness of the hybrid metaheuristic algorithm, we conducted comparative experiments against three commonly used scheduling rules in practice: max-power immediate charging (MPIC), max-power delayed charging (MPDC), and

average-power immediate charging (APIC). The MPIC is straightforward and widely adopted—it charges EVs at maximum power upon arrival until charging demand is met. The MPDC delays charging for a period of time after the EV arrives and then charges it at the maximum power, ensuring that the demand is met at the expected departure time. This rule is suitable for scenarios where EVs arrive within a concentrated time window but depart at staggered intervals. The APIC charges EVs at a constant average power throughout their parking duration, ensuring that the charging demand is fully met by the time of departure. It represents a more balanced strategy. In addition, we designed a BESS scheduling rule to operate alongside the above EV scheduling rules. Specifically, the BESS discharges at maximum power when no future time periods have higher electricity prices, charges at maximum power during the lowest-price time periods, and remains idle during other periods. This rule enables the BESS to effectively exploit the time-of-use electricity price gap, thereby enhancing the overall performance of the scheduling rules.

In the experiments, we generated 10 instances using relevant probability distributions for each above-mentioned scenario. For each instance, we applied the hybrid metaheuristic algorithm 10 times and used the average objective function value as the performance indicator to mitigate randomness. The results are presented in Table and Figure 7. In each scenario, we carry out separate paired Wilcoxon signed-rank tests of the hybrid metaheuristic algorithm against MPIC, MPDC, and APIC, respectively, and each comparison returned an exact p-value of 0.00195, confirming significant differences. The results illustrate that the hybrid metaheuristic algorithm consistently outperformed all scheduling rules across all scenarios, with cost reductions ranging from 28.60% to 68.72%. Moreover, as the number of users decreases, the hybrid metaheuristic algorithm's advantage grows. This is because, in scenarios with fewer users, total demand is lower, allowing the BESS to discharge more energy to the grid. This enlarges the optimization space and reduces operational costs. Similarly, the algorithm performs better in scenarios with longer average parking durations, as extended parking durations provide more discharging opportunities for both EVs and

BESS.

Table 9 Performance comparison of hybrid metaheuristic with scheduling rules in multiple scenarios

Instance	Hybrid metaheuristic		MPIC	MPDC	APIC
	Average	Best			
SU-MD-1	261.45	260.80	403.22	681.44	525.78
SU-MD-2	297.58	297.58	384.45	620.64	524.68
SU-MD-3	259.37	259.37	425.43	651.69	554.73
SU-MD-4	128.11	128.11	234.16	605.85	381.80
SU-MD-5	259.07	259.07	338.50	648.27	517.84
SU-MD-6	213.85	213.85	352.06	737.76	544.98
SU-MD-7	71.35	71.35	200.98	451.39	327.19
SU-MD-8	315.78	315.78	377.95	622.55	508.20
SU-MD-9	275.83	275.83	423.74	720.01	569.89
SU-MD-10	306.55	306.55	379.33	687.77	552.14
MU-MD-1	282.30	280.77	471.72	805.63	643.49
MU-MD-2	371.93	371.93	496.62	610.40	555.59
MU-MD-3	330.22	328.83	430.39	766.71	580.75
MU-MD-4	301.40	301.20	451.04	793.29	590.91
MU-MD-5	222.44	222.44	363.84	561.17	476.51
MU-MD-6	248.16	248.00	356.94	632.25	450.42
MU-MD-7	281.21	279.49	450.45	790.33	613.87
MU-MD-8	307.23	307.23	384.72	628.11	481.44
MU-MD-9	326.63	326.09	462.91	787.97	584.82
MU-MD-10	373.64	373.64	507.40	835.10	671.62
LU-MD-1	277.43	277.43	388.34	643.76	474.16
LU-MD-2	332.04	332.04	506.37	781.48	624.87
LU-MD-3	419.01	416.58	604.37	824.37	686.26
LU-MD-4	444.32	444.12	546.85	842.39	656.10
LU-MD-5	415.13	411.69	533.18	784.45	632.21
LU-MD-6	470.25	470.25	638.10	985.51	779.41
LU-MD-7	463.58	463.58	563.63	806.85	684.26
LU-MD-8	492.11	491.20	688.16	1006.35	769.96
LU-MD-9	160.81	160.81	369.76	590.92	486.41
LU-MD-10	258.52	258.15	390.05	660.77	482.34
SU-SD-1	236.56	236.03	294.36	646.21	463.75
SU-SD-2	249.31	246.96	338.95	538.74	422.41
SU-SD-3	239.01	239.01	342.48	577.45	429.73
SU-SD-4	228.49	228.49	316.28	620.83	453.06
SU-SD-5	250.33	250.33	346.68	650.36	496.32
SU-SD-6	268.37	267.81	380.51	676.09	505.21
SU-SD-7	247.96	247.96	413.45	663.56	500.78
SU-SD-8	194.18	194.18	322.41	610.34	455.99
SU-SD-9	409.82	409.82	541.86	815.05	644.40
SU-SD-10	185.97	185.97	297.39	601.63	437.44
SU-LD-1	24.68	24.68	226.83	452.44	387.30
SU-LD-2	236.16	236.16	309.39	492.33	448.89
SU-LD-3	130.05	130.05	256.58	523.28	388.77
SU-LD-4	114.91	114.91	252.08	508.61	395.27
SU-LD-5	117.29	117.29	293.57	537.39	421.75
SU-LD-6	217.43	217.43	362.51	614.47	488.74
SU-LD-7	202.65	202.65	331.03	523.95	466.04
SU-LD-8	229.49	227.09	322.00	622.60	508.89
SU-LD-9	108.30	107.00	270.10	530.65	437.10
SU-LD-10	313.01	313.01	403.52	610.09	501.30

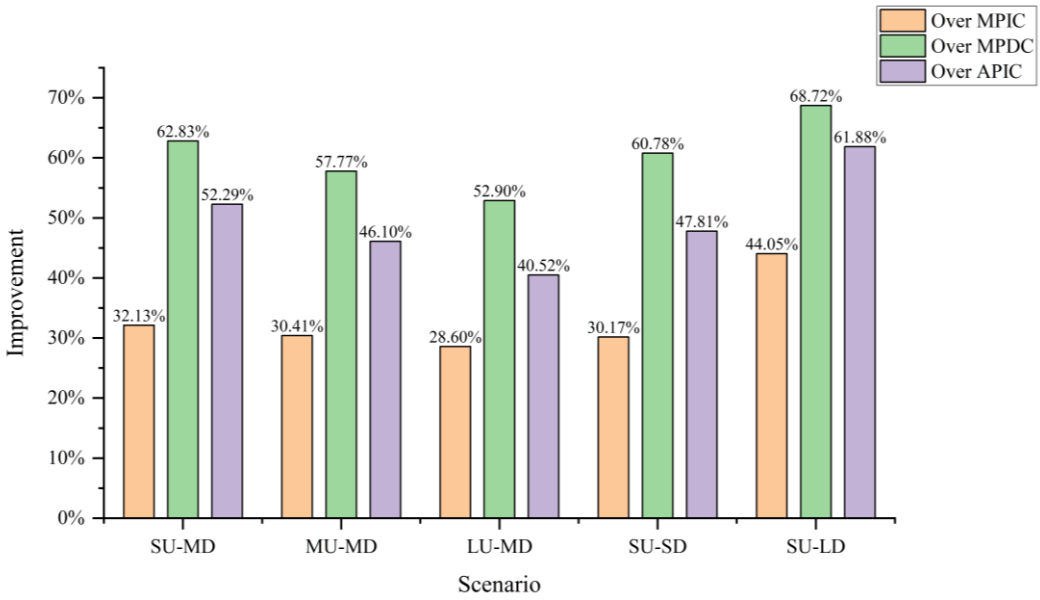

Figure 7 Improvement of hybrid metaheuristic algorithm over scheduling rules

5.3.4 Comparative and statistical analysis of metaheuristic algorithms

To provide a more comprehensive assessment of the role of PSO in the proposed hybrid metaheuristic algorithm, we conducted additional comparative experiments with two established metaheuristics, namely genetic algorithm (GA) and simulated annealing (SA). GA is a representative population-based metaheuristic that explores the solution space through evolutionary operations on a population of candidate solutions, whereas SA is a representative trajectory-based metaheuristic that explores the search space through stochastic neighborhood moves and probabilistic acceptance. The inclusion of these two algorithms therefore enables the performance of PSO to be assessed against different search paradigms under the same problem setting.

For the GA benchmark, the algorithm design and parameter settings were established with reference to the GA implementations in Abreu et al. (2020) and D'Angelo and Palmieri (2021), with appropriate adaptations to the problem considered in this study. Each individual is encoded as a vector representing the BESS charging and discharging powers over the remaining time periods, while the EV charging schedule is generated by the same greedy strategy used in the proposed framework. To enhance the quality and diversity of the initial population, the MPIC, MPDC, and APIC

schedules introduced in Section 5.3.3 are incorporated as seed solutions, and the remaining individuals are generated by perturbing these solutions. During evolution, tournament selection is adopted to choose parents, followed by arithmetic crossover that combines the corresponding BESS power values of the selected parents. Mutation is then applied by randomly perturbing individual power values within the feasible range to maintain population diversity. An elitist strategy is used to preserve high-quality individuals. The resulting individuals are evaluated using the same objective function and feasibility-handling mechanism as those used in the PSO-based framework, thereby providing a consistent basis for comparison.

For the SA benchmark, its algorithmic design and parameter configuration were guided by the implementations reported in Ali et al. (2002) and Franzin and Stützle (2023), with problem-specific adaptations incorporated for the present study. The same solution representation and EV scheduling strategy as in GA are adopted. The initial solution is selected from the greedy and rule-based schedules (MPIC, MPDC, APIC) according to their objective values. At each iteration, a neighboring solution is generated by perturbing the BESS power values of one to three randomly selected time periods. An improving solution is directly accepted, while a non-improving solution may still be accepted depending on its objective deterioration and the current temperature, with the likelihood of acceptance gradually decreasing as the temperature is reduced. The best solution encountered throughout the search is retained as the final solution.

To conduct the comparative experiments, four instances from each of the five scenarios, namely SU-MD, MU-MD, LU-MD, SU-SD, and SU-LD, were considered, resulting in a total of 20 test instances. PSO, GA, and SA were independently executed 10 times on each instance to account for the stochastic nature of the metaheuristic algorithms. The computational results are summarized in Table 10, where Best and Average report the best and average objective values obtained over the 10 independent runs, respectively, and T (s) denotes the average computational time in seconds over these runs.

Table 10 Performance comparison of PSO, GA, and SA on the test instances

Instance	PSO			GA			SA		
	Average	Best	T (s)	Average	Best	T (s)	Average	Best	T (s)
SU-MD-E1	14.33	14.33	317.22	113.95	113.95	1400.55	209.88	209.88	431.31
SU-MD-E2	116.59	113.47	317.31	243.16	242.44	1122.30	267.08	267.05	519.69
SU-MD-E3	213.13	211.41	322.69	311.21	311.21	1125.01	374.72	374.72	591.64
SU-MD-E4	19.13	19.13	355.45	102.91	102.91	2008.70	236.62	236.62	1006.17
MU-MD-E1	233.05	230.22	428.29	298.77	298.62	1068.07	385.36	385.30	600.88
MU-MD-E2	57.76	56.73	458.27	92.91	92.91	1356.90	238.92	238.92	461.12
MU-MD-E3	68.62	67.89	516.37	102.90	102.25	1885.53	257.36	257.28	624.32
MU-MD-E4	166.76	166.64	472.23	222.26	222.26	1796.85	351.92	351.92	776.92
LU-MD-E1	210.61	206.77	617.66	250.92	249.98	1309.38	366.27	366.27	830.91
LU-MD-E2	90.59	90.59	616.06	107.26	107.26	2418.74	301.34	301.33	1013.00
LU-MD-E3	168.78	168.78	560.68	165.72	165.72	825.92	253.29	253.29	344.78
LU-MD-E4	186.75	180.56	619.17	222.44	222.44	1382.36	390.29	390.29	753.22
SU-SD-E1	54.43	54.43	338.49	197.26	197.26	1811.95	276.11	276.11	985.06
SU-SD-E2	264.23	261.16	265.99	380.30	380.30	734.47	363.82	363.82	529.86
SU-SD-E3	103.20	101.02	320.14	166.68	166.68	1639.16	288.08	288.08	795.91
SU-SD-E4	137.32	137.32	377.59	249.00	249.00	1256.35	337.15	337.15	846.46
SU-LD-E1	101.03	101.03	392.62	142.76	142.76	1842.13	319.64	319.64	819.28
SU-LD-E2	181.64	181.64	306.59	215.78	215.78	1151.26	308.87	308.87	634.84
SU-LD-E3	40.08	37.77	388.09	59.90	59.90	1587.34	172.39	172.39	561.08
SU-LD-E4	178.71	178.68	321.68	177.71	177.71	1390.11	330.20	329.94	633.22

As shown in Table 10, PSO achieved better solutions than GA in 18 out of the 20 test instances, while GA obtained better solutions in the remaining two instances. Compared with SA, PSO consistently outperformed SA on all tested instances. In addition to solution quality, PSO also exhibited lower computational times than GA and SA, demonstrating higher computational efficiency. On average, PSO reduced the operational costs by 33.99% and 59.36% compared with GA and SA, respectively. The superior performance of PSO can be attributed to its suitability for the continuous optimization characteristics of the considered problem. In this study, the decision variables optimized by the metaheuristic algorithms are the charging and discharging powers of the BESS over multiple time periods, which form a high-dimensional continuous search space. PSO directly updates particle positions and velocities in this continuous space while exploiting the information shared among particles through

personal and global best solutions, enabling an effective balance between exploration and exploitation. This search mechanism is particularly suitable for continuously adjusting BESS power schedules within the rolling horizon framework.

GA also achieved better performance than SA on most instances. This difference can be explained by the distinct search mechanisms of the two algorithms. GA maintains a population of candidate solutions and utilizes crossover operations to combine information from different individuals, thereby improving the exploration capability of the search process. In contrast, SA explores the solution space through a single trajectory and relies on neighborhood perturbations and probabilistic acceptance, which may limit its ability to explore diverse regions of the search space within the same computational budget. Nevertheless, both GA and SA achieved substantial improvements over conventional scheduling rules, demonstrating their effectiveness in optimizing BESS scheduling. Specifically, compared with MPIC, the best-performing scheduling rule, GA and SA reduced the average operational cost by 40.01% and 2.31%, respectively.

To statistically verify the observed performance differences among PSO, GA, and SA, the Friedman test and pairwise Wilcoxon signed-rank tests were conducted based on the average objective values obtained from the 20 test instances. The Friedman test produced a chi-square statistic of 34.3 with a p-value of 3.563×10^{-8}, indicating statistically significant differences among the three metaheuristic algorithms. Moreover, PSO achieved the lowest average rank of 1.10, followed by GA (1.95) and SA (2.95), confirming its superior overall performance. Pairwise Wilcoxon signed-rank tests were further performed to identify the significance of the performance differences between algorithms. The comparisons between PSO and GA, PSO and SA, and GA and SA yielded p-values of 4.768×10^{-6}, 9.537×10^{-7}, and 1.907×10^{-6}, respectively. After Holm correction for multiple comparisons, all adjusted p-values remained below 0.001, demonstrating that the performance differences among the three algorithms are statistically significant. These results provide statistical evidence that the proposed PSO optimization approach achieves superior solution quality compared with alternative

metaheuristic approaches.

6. Conclusions

This paper investigates the UPEM problem, aiming to minimize operating costs by optimizing the charging and discharging powers of EVs and the BESS across different time periods. We fully consider user preferences to satisfy both time-sensitive and price-sensitive users and thus improve user satisfaction. Furthermore, we introduce BESS and V2G technology and integrate the BESS capacity with the energy management schedule for integrated optimization. This integration further enhances BESS utilization and reduces operating costs. To address this problem, we decompose the dynamic scheduling problem into a series of static subproblems and propose a hybrid metaheuristic algorithm to solve them. The hybrid metaheuristic algorithm combines a greedy algorithm with the PSO algorithm. Specifically, the greedy algorithm generates charging and discharging schedules for EVs by prioritizing charging during low electricity price periods and discharging during high electricity price periods. Meanwhile, the PSO algorithm performs a global search to optimize the BESS charging and discharging schedule based on the EV schedules and the BESS energy state. Moreover, we incorporate a dominance-based correction rule into the PSO algorithm to repair poor solutions and thus enhance algorithm performance.

In the experimental section, we design various scenarios with different number of users and parking durations to validate the algorithm's applicability. The results demonstrate that introducing V2G and BESS reduces operating costs. In particular, the integration of V2G with the greedy algorithm lowers the operating cost by an average of 22.91%. By further introducing the BESS and optimizing its charging and discharging power with the PSO algorithm, the cost is further reduced by an average of 17.71% across all scenarios. Moreover, the hybrid metaheuristic algorithm outperforms the commonly used scheduling rules—MPIC, MPDC, and APIC. It achieves cost reductions ranging from 28.60% to 68.72% across all scenarios. Furthermore, comparative experiments with two representative metaheuristics, namely GA and SA, demonstrate the superior performance of the proposed PSO-based hybrid metaheuristic

algorithm in terms of both solution quality and computational efficiency. The statistical analysis further confirms that the performance improvements are statistically significant. These results fully demonstrate the broad applicability and superiority of our hybrid metaheuristic algorithm in different scenarios.

Future research can be extended in two directions. First, we assume that users can accurately determine their parking duration before charging. In practice, parking duration may be uncertain due to external factors. For example, users visiting a hospital may face unpredictable parking durations because of patient flow, doctor efficiency, and case complexity. Therefore, future work could investigate how to optimize charging schedules under uncertain parking durations to improve the charging station's adaptability to various conditions. Second, this paper focuses on two energy supply technologies for the charging station—V2G and BESS. Future studies could consider additional energy supply options, such as photovoltaic and wind power, to diversify the station's energy sources. This diversification could further reduce operating costs and enhance sustainability.

CRediT authorship contribution statement

Wenjie Hu: Conceptualization. Methodology, Software, Validation, Writing - review & editing. **Jiamou Su**: Conceptualization, Methodology, Software, Validation, Formal analysis, Investigation, Visualization, Writing - original draft. **Yang Wang**: Supervision, Conceptualization, Writing - review & editing, Project administration, Funding acquisition. **Ya-Hui Jia**: Supervision, Writing - review & editing, Conceptualization. **Wei-Neng Chen**: Supervision, Conceptualization, Resources, Project administration, Funding acquisition. **Jin-Kao Hao**: Supervision, Conceptualization, Resources.

Declaration of generative AI and AI-assisted technologies in the writing process

During the preparation of this work, the authors used ChatGPT in order to improve the readability and language of the manuscript. After using this tool, the authors

reviewed and edited the content as needed and take full responsibility for the content of the published article.

Declaration of competing interest

The authors declare that they have no known competing financial interests or personal relationships that could have appeared to influence the work reported in this paper.

Data availability

The authors declare that the input data supporting the findings of this study are available within the paper. Further inquiries regarding the data can be directed to the corresponding author.

Acknowledgements

The authors would like to thank the reviewers for their insightful comments and constructive suggestions, which contributed to improving the quality of this manuscript. This work was supported in part by the National Key Research and Development Project No. 2023YFE0206200.

References

Abdelfattah, W., Abdelhamid, A. S., Hasanien, H. M., & Rashad, B. A.-E. (2024). Smart vehicle-to-grid integration strategy for enhancing distribution system performance and electric vehicle profitability. *Energy*, *302*, 131807. https://doi.org/10.1016/j.energy.2024.131807

Abreu, L. R., Cunha, J. O., Prata, B. A., & Framinan, J. M. (2020). A genetic algorithm for scheduling open shops with sequence-dependent setup times. *Computers & Operations Research*, *113*, 104793. https://doi.org/10.1016/j.cor.2019.104793

Alaee, P., Bems, J., & Anvari-Moghaddam, A. (2023). A review of the latest trends in technical and economic aspects of EV charging management. *Energies*, *16*(9),

3669. https://doi.org/10.3390/en16093669

Ali, M. M., Törn, A., & Viitanen, S. (2002). A direct search variant of the simulated annealing algorithm for optimization involving continuous variables. *Computers & Operations Research*, *29*(1), 87–102. https://doi.org/10.1016/S0305-0548(00)00064-2

Aliasghari, P., Mohammadi-Ivatloo, B., Alipour, M., Abapour, M., & Zare, K. (2018). Optimal scheduling of plug-in electric vehicles and renewable micro-grid in energy and reserve markets considering demand response program. *Journal of Cleaner Production*, *186*, 293–303. https://doi.org/10.1016/j.jclepro.2018.03.058

Amini, M., Nazari, M. H., & Hosseinian, S. H. (2023). Optimal energy management of battery with high wind energy penetration: A comprehensive linear battery degradation cost model. *Sustainable Cities and Society*, *93*, 104492. https://doi.org/10.1016/j.scs.2023.104492

Bhatti, A. R., Salam, Z., Sultana, B., Rasheed, N., Awan, A. B., Sultana, U., & Younas, M. (2019). Optimized sizing of photovoltaic grid-connected electric vehicle charging system using particle swarm optimization. *International Journal of Energy Research*, *43*(1), 500–522. https://doi.org/10.1002/er.4287

Bibak, B., & Tekiner-Moğulkoç, H. (2021). A comprehensive analysis of vehicle to grid (V2G) systems and scholarly literature on the application of such systems. *Renewable Energy Focus*, *36*, 1–20. https://doi.org/10.1016/j.ref.2020.10.001

Çakıl, F., & Aksoy, N. (2025). Reinforcement learning-based multi-objective smart energy management for electric vehicle charging stations with priority scheduling. *Energy*, *322*, 135475. https://doi.org/10.1016/j.energy.2025.135475

Cao, Y., Tang, S., Li, C., Zhang, P., Tan, Y., Zhang, Z., & Li, J. (2012). An optimized EV charging model considering TOU price and SOC curve. *IEEE Transactions on Smart Grid*, *3*(1), 388–393. https://doi.org/10.1109/TSG.2011.2159630

Christensen, T. H., Friis, F., Bettin, S., Throndsen, W., Ornetzeder, M., Skjølsvold, T. M., & Ryghaug, M. (2020). The role of competences, engagement, and devices

in configuring the impact of prices in energy demand response: Findings from three smart energy pilots with households. *Energy Policy*, *137*, 111142. https://doi.org/10.1016/j.enpol.2019.111142

Dai, Q., Liu, J., & Wei, Q. (2019). Optimal photovoltaic/battery energy storage/electric vehicle dharging station design based on multi-agent particle swarm optimization algorithm. *Sustainability*, *11*(7), 1973. https://doi.org/10.3390/su11071973

D'Angelo, G., & Palmieri, F. (2021). GGA: A modified genetic algorithm with gradient-based local search for solving constrained optimization problems. *Information Sciences*, *547*, 136–162. https://doi.org/10.1016/j.ins.2020.08.040

Domínguez-Navarro, J. A., Dufo-López, R., Yusta-Loyo, J. M., Artal-Sevil, J. S., & Bernal-Agustín, J. L. (2019). Design of an electric vehicle fast-charging station with integration of renewable energy and storage systems. *International Journal of Electrical Power & Energy Systems*, *105*, 46–58. https://doi.org/10.1016/j.ijepes.2018.08.001

Feng, H. J., Xi, L. C., Jun, Y. Z., Ling, Y. X., & Jun, H. (2020). Review of electric vehicle charging demand forecasting based on multi-source data. *2020 IEEE Sustainable Power and Energy Conference (iSPEC)*, 139–146. https://doi.org/10.1109/iSPEC50848.2020.9351008

Franzin, A., & Stützle, T. (2023). A landscape-based analysis of fixed temperature and simulated annealing. *European Journal of Operational Research*, *304*(2), 395–410. https://doi.org/10.1016/j.ejor.2022.04.014

García-Álvarez, J., González, M. A., & Vela, C. R. (2018). Metaheuristics for solving a real-world electric vehicle charging scheduling problem. *Applied Soft Computing*, *65*, 292–306. https://doi.org/10.1016/j.asoc.2018.01.010

Guner, S., & Ozdemir, A. (2017). Stochastic energy storage capacity model of EV parking lots. *IET Generation, Transmission & Distribution*, *11*(7), 1754–1761. https://doi.org/10.1049/iet-gtd.2016.1406

Han Z. (2024). *Considering the hybrid energy storage capacity configuration for*

electric vehicle charging load (in Chinese) [Master's thesis, Shaanxi University of Technology]. https://doi.org/10.27733/d.cnki.gsxlg.2024.000318

Hannan, M. A., Hoque, M. M., Mohamed, A., & Ayob, A. (2017). Review of energy storage systems for electric vehicle applications: Issues and challenges. *Renewable and Sustainable Energy Reviews*, *69*, 771–789. https://doi.org/10.1016/j.rser.2016.11.171

Honarmand, M., Zakariazadeh, A., & Jadid, S. (2014). Optimal scheduling of electric vehicles in an intelligent parking lot considering vehicle-to-grid concept and battery condition. *Energy*, *65*, 572–579. https://doi.org/10.1016/j.energy.2013.11.045

Jia, Z., Li, J., Zhang, X.-P., & Zhang, R. (2023). Review on optimization of forecasting and coordination strategies for electric vehicle charging. *Journal of Modern Power Systems and Clean Energy*, *11*(2), 389–400. https://doi.org/10.35833/MPCE.2021.000777

Juneja, M., & Nagar, S. K. (2016). Particle swarm optimization algorithm and its parameters: A review. *2016 International Conference on Control, Computing, Communication and Materials (ICCCCM)*, 1–5. https://doi.org/10.1109/ICCCCM.2016.7918233

Lai, C. S., Chen, D., Zhang, J., Zhang, X., Xu, X., Taylor, G. A., & Lai, L. L. (2022). Profit maximization for large-scale energy storage systems to enable fast EV charging infrastructure in distribution networks. *Energy*, *259*, 124852. https://doi.org/10.1016/j.energy.2022.124852

Li, D., Zouma, A., Liao, J. T., & Yang, H. T. (2020). An energy management strategy with renewable energy and energy storage system for a large electric vehicle charging station. *eTransportation*, *6*, 100076. https://doi.org/10.1016/j.etran.2020.100076

Liu, N., Zou, F., Wang, L., Wang, C., Chen, Z., & Chen, Q. (2016). Online energy management of PV-assisted charging station under time-of-use pricing. *Electric Power Systems Research*, *137*, 76–85.

https://doi.org/10.1016/j.epsr.2016.04.002

Mahmud, I., Medha, M. B., & Hasanuzzaman, M. (2023). Global challenges of electric vehicle charging systems and its future prospects: A review. *Research in Transportation Business & Management*, *49*, 101011. https://doi.org/10.1016/j.rtbm.2023.101011

Mohamed, A., & Mohammed, O. (2013). Real-time energy management scheme for hybrid renewable energy systems in smart grid applications. *Electric Power Systems Research*, *96*, 133–143. https://doi.org/10.1016/j.epsr.2012.10.015

Mohamed, A., Salehi, V., Ma, T., & Mohammed, O. (2014). Real-time energy management algorithm for plug-In hybrid electric vehicle charging parks involving sustainable energy. *IEEE Transactions on Sustainable Energy*, *5*(2), 577–586. https://doi.org/10.1109/TSTE.2013.2278544

Pan, K., Liang, C. D., & Lu, M. (2024). Optimal scheduling of electric vehicle ordered charging and discharging based on improved gravitational search and particle swarm optimization algorithm. *International Journal of Electrical Power & Energy Systems*, *157*, 109766. https://doi.org/10.1016/j.ijepes.2023.109766

Shami, T. M., El-Saleh, A. A., Alswaitti, M., Al-Tashi, Q., Summakieh, M. A., & Mirjalili, S. (2022). Particle swarm optimization: A comprehensive survey. *IEEE Access*, *10*, 10031–10061. https://doi.org/10.1109/ACCESS.2022.3142859

Shi, Y., & Eberhart, R. C. (1999). Empirical study of particle swarm optimization. *Proceedings of the 1999 Congress on Evolutionary Computation-CEC99 (Cat. No. 99TH8406)*, 1945–1950. https://doi.org/10.1109/CEC.1999.785511

Viegas, M. A. A., & Da Costa, C. T. (2021). Fuzzy logic controllers for charging/discharging management of battery electric vehicles in a smart grid. *Journal of Control, Automation and Electrical Systems*, *32*(5), 1214–1227. https://doi.org/10.1007/s40313-021-00741-w

Yang, S., Tan, Z., Lin, H., Li, P., De, G., Zhou, F., & Ju, L. (2020). A two-stage optimization model for Park Integrated Energy System operation and benefit

allocation considering the effect of Time-Of-Use energy price. *Energy*, *195*, 117013. https://doi.org/10.1016/j.energy.2020.117013

Yao, L., Lim, W. H., & Tsai, T. S. (2017). A real-time charging scheme for demand response in electric vehicle parking station. *IEEE Transactions on Smart Grid*, *8*(1), 52–62. https://doi.org/10.1109/TSG.2016.2582749

Yuan, M., Zhang, H., Wang, B., Huang, L., Fang, K., & Liang, Y. (2020). Downstream oil supply security in China: Policy implications from quantifying the impact of oil import disruption. *Energy Policy*, *136*, 111077. https://doi.org/10.1016/j.enpol.2019.111077

Zhang, H., Song, X., Xia, T., Yuan, M., Fan, Z., Shibasaki, R., & Liang, Y. (2018). Battery electric vehicles in Japan: Human mobile behavior based adoption potential analysis and policy target response. *Applied Energy*, *220*, 527–535. https://doi.org/10.1016/j.apenergy.2018.03.105

Zhou, K., Wei, S., & Yang, S. (2019). Time-of-use pricing model based on power supply chain for user-side microgrid. *Applied Energy*, *248*, 35–43. https://doi.org/10.1016/j.apenergy.2019.04.076

Zhu, L., Wang, P., & Zhang, Q. (2019). Indirect network effects in China's electric vehicle diffusion under phasing out subsidies. *Applied Energy*, *251*, 113350. https://doi.org/10.1016/j.apenergy.2019.113350